Effects of Novel Polymorphisms in the RAGE Gene on Transcriptional Regulation and Their Association With Diabetic Retinopathy

Barry I. Hudson, Max H. Stickland, T. Simon Futers, and Peter J. Grant

Interactions between advanced glycation end products (AGEs) and the receptor for AGE (RAGE) are implicated in the vascular complications in diabetes. We have identified eight novel polymorphisms, of which the −1420 (GGT)n, −1393 G/T, −1390 G/T, and −1202 G/A were in the overlapping PBX2 3′ untranslated region (UTR), and the −429 T/C (66.5% TT, 33.5% TC/CC), −407 to −345 deletion (99% I, 1% I/D, 0% D), −374 T/A (66.4% TT, 33.6% TA/AA), and +20 T/A were in the RAGE promoter. To evaluate the effects on transcriptional activity, we measured chloramphenicol acetyl transferase (CAT) reporter gene expression, driven by variants of the −738 to +49 RAGE gene fragment containing the four polymorphisms identified close to the transcriptional start site. The −429 C, −374 A, and 63-bp deletion alleles resulted in a mean increase of CAT expression of twofold ($P < 0.0001$), threefold ($P < 0.001$), and fourfold ($P < 0.05$), respectively, with the −374 T and A alleles yielding highly differential binding of nuclear protein extract from both monocyte- and hepatocyte-derived cell lines. The prevalence of the functional polymorphisms were investigated in subjects with type 2 diabetes (106 with and 109 without retinopathy), with the −429 C allele showing an increase in the retinopathy group ($P < 0.05$). These data suggest that the polymorphisms involved in differences in RAGE gene regulation may influence the pathogenesis of diabetic vascular complications. *Diabetes* 50:1505–1511, 2001

The major complications associated with diabetes are diseases of the macro- and microvasculature, which have been postulated to be related to the formation of advanced glycation end products (AGEs). AGEs result from the nonenzymatic glycation of proteins and lipids (1), which form during aging and at an accelerated rate in diabetes as a result of hyperglycemia.

AGEs produce a plethora of effects through a number of mechanisms. Firstly, AGEs form on the extracellular matrix, altering vascular structure and trapping circulatory proteins, leading to a narrowing of the lumen (1,2). Secondly, AGEs form on intracellular proteins and DNA, resulting in cellular changes. Thirdly, the principle means of derangement of AGEs is by specific AGE-binding receptors, which include the AGE-receptor complex (3), the macrophage scavenger receptors (4), and the receptor for AGE (RAGE) (5). The receptor most supported by studies is RAGE, a member of the immunoglobulin superfamily. The gene for RAGE is found on chromosome 6p21.3 in the MHC locus and is composed of a 1.7-kb 5′ flanking region and 11 exons (6). RAGE is normally expressed at low levels by the endothelium, smooth muscle, mesangial, and monocytes (7), but in both animal models and human diabetic subjects, high levels of RAGE expression have been identified in the retina, mesangial, and aortic vessels, concomitant with AGE accumulation (8,9).

In normal homeostasis, it appears that RAGE functions to bind and internalize low levels of AGE for degradation; however, in diabetes, because of the sustained interaction of higher levels of AGEs, this appears to lead to receptor-mediated activation and secretion of various cytokines (10). These induce a cascade of protein expression (10), among which increased tissue factor (11) and fibrinolytic inhibitor plasminogen-activator inhibitor-1 (12) expression promote a procoagulant state. Further endothelial dysfunction is brought about by the recruitment of monocytes via a RAGE-dependent mechanism to these sites of AGE accumulation (13). From in vitro studies, it appears that a feedback loop of increasing expression of RAGE, via nuclear factor–κβ, results from AGE-RAGE binding to enhance these effects (10).

Inherited differences in key transcription binding sites involved in RAGE gene regulation could alter this pathway of events by either increasing or decreasing RAGE expression. To investigate for the presence of novel polymorphisms in the RAGE 5′ flanking region, we screened the entire 5′ gene regulatory region of RAGE for novel polymorphisms using a combination of single-strand conformation polymorphism (SSCP) and denaturing high-performance liquid chromatography (DHPLC). Because of the dense nature of genes within the MHC locus, part of the 5′ flanking region of RAGE overlaps with the 3′ untranslated region (UTR) of the PBX2 gene (6), further complicating the correct identification of polymorphisms due to the presence of a pseudogene copy of PBX2 on

chromosome 3. Correctly identified polymorphisms were functionally characterized by transient transfection assays using RAGE promoter regions to drive the chloramphenicol acetyl transferase (CAT) reporter gene, and nuclear protein interactions were characterized by electrophoretic mobility shift assays (EMSA). Functionally active polymorphisms were assessed for their prevalence in a control population and in subjects with type 2 diabetes with and without retinopathy.

RESEARCH DESIGN AND METHODS

Initial polymerase chain reaction (PCR) optimizations were performed using DNA from anonymous blood donors that was previously obtained from the British Blood Transfusion Service Center, Leeds, U.K. Subsequent mutation detection was carried out with DNA from 80 random blood donors. Genotype frequencies were investigated in subjects with type 2 diabetes with ($n = 106$) and without ($n = 109$) retinopathy who were previously recruited from the outpatient clinic at the General Infirmary, Leeds. Type 2 diabetes was diagnosed according to World Health Organization criteria. Retinopathy was defined by opthalmoscopic examination performed by an opthamologist with special interest in diabetic retinal disease. Subjects were classified as previously described (14). Each subject gave informed consent, and the study was approved by the United Leeds Teaching Hospitals (National Health Service) Trust Research Ethics Committee. Human genomic DNA was obtained from 10 ml of whole blood in EDTA using the Nucleon extraction kit (Nucleon Biosciences).

PCR. All available genomic sequences for human RAGE 5′ flanking region were obtained from the internet site www3.ncbi.nlm.nih.gov/. RAGE sequences U89336, AF001095, and D28769 were aligned using ClustalW at the Internet site www2.ebi.ac.uk/clustalw/ to determine discrepancies among sequences for successful primer design. Primers were designed to overlap each promoter region and were synthesized (Life Technologies). All primer sequences and conditions are available from the authors. PCRs consisted of a 25-µl reaction volume containing 25 pmol of forward and reverse primer, 100 ng of template DNA, 200 µmol/l of each deoxynucleotide phosphate, 1–2 mmol/l MgCl$_2$, 0.6 U Taq DNA polymerase (Life Technologies), and a reaction buffer containing 20 mmol/l Tris-HCl, 50 mmol/l KCl, 0.05% W1 (Life Technologies). Amplification consisted of 30 cycles of 94°C for 1 min, a primer-annealing step of 56–58°C for 1 min, and primer extension at 72°C for 1 min, followed by a final extension for 5 min at 72°C.

SSCP. Each primer set was used to amplify DNA ($\sim$190–230 bp) from 80 individuals. A total of 5 µl of PCR product was diluted in 14 µl of SSCP loading buffer (95% formamide, 20 mmol/l EDTA, 0.025% bromophenol blue, and xylene cyanol), heated to 100°C for 10 min, and placed on ice. Adjacent promoter regions differing $\sim$100 bp in size were simultaneously loaded on a vertical 0.75× Mutation Detection Enhancement gel (Flowgen) with +/−10% glycerol by first loading the smaller fragment and electrophoresing it into the gel for 1 h and then adding the larger promoter region. Gels were run at either room temperature overnight at 9W or 4°C for 4 h at 40W and DNA visualized using a previously published silver staining method (15).

DHPLC. Samples were run on an ion-pairing reverse-phase HPLC system (Transgenomic) fitted with a DNASep column. Primer sets were used in combination to amplify a PCR product of $\sim$350 bp from 80 individuals, as previously described. The coupling reagent was tri-ethyl ammonium acetate (TEAA), and the gradient was achieved with acetonitrile. Buffer A consisted of 0.1 mol/l TEAA and buffer B consisted of 0.1 mol/l TEAA with 25% acetonitrile. A total of 5 µl of PCR product was run on a 16-min gradient of 40–72% buffer B (2% change per min) at 50°C. Fragment purity and size could be verified by the presence of a single peak without a shoulder and by the retention time. The latter was used to calculate a 6.5-min optimized gradient with a 13% change of buffer B such that the fragment was eluted at $\sim$6–6.5 min. Aliquots of the same sample were injected onto the column on the optimized gradient at 1°C intervals from 50 to 70°C. From a plot of retention time against temperature, the screening conditions could be selected. If any of the selected screening temperatures had a retention time of <5 min, the gradient was altered to move the peak to $\sim$5–6 min. The PCR products for screening were heteroduplexed by heating to 95°C for 5 min and slowly cooling to 25°C over 45 min. The PCR samples were injected onto the column and DHPLC was performed using the previously determined conditions. To identify potential heterozygous samples, results were analyzed by overlaying chromatograms.

DNA sequencing. The presence of a pseudogene for the 5′ end of the RAGE promoter necessitated primers (RPALL) designed to specifically amplify from chromosome 6 alone (RPALL F 5′ TTGTATGCTCTGGAATCTGTGG 3′ RPALL R 5′ CTCTGTCTGCCCCTCTCCCT 3′). Samples were amplified using Expand

High Fidelity PCR system (Roche) using 2.6 U Expand enzyme mix, 200 µmol/l dNTPs, and 1.5 mmol/l Mg^{2+} in High Fidelity Expand buffer. Amplification consisted of 94°C for 2 min, 10 cycles of 94°C for 15 s, 58°C for 30 s, 72°C for 2 min, 20 cycles of 94°C for 15 s, 58°C for 30 s, 72°C for 2 min increasing 5 s a cycle, and a final extension at 72°C for 5 min. PCR fragments were gel purified using a NucleoSpin (Macherey Nagel) kit, and nested PCR was performed to amplify each specific region. PCR products were purified using QuickStep PCR purification columns (EDGE Biosystems), and cycle sequencing reactions were set-up with BigDye Ready Reaction mix (Applied Biosystems) according to manufacturers instructions. Purification was carried out using AGTC Centriflex gel filtration columns (EDGE Biosystems) before automated sequencing on an ABI310 (Applied Biosystems).
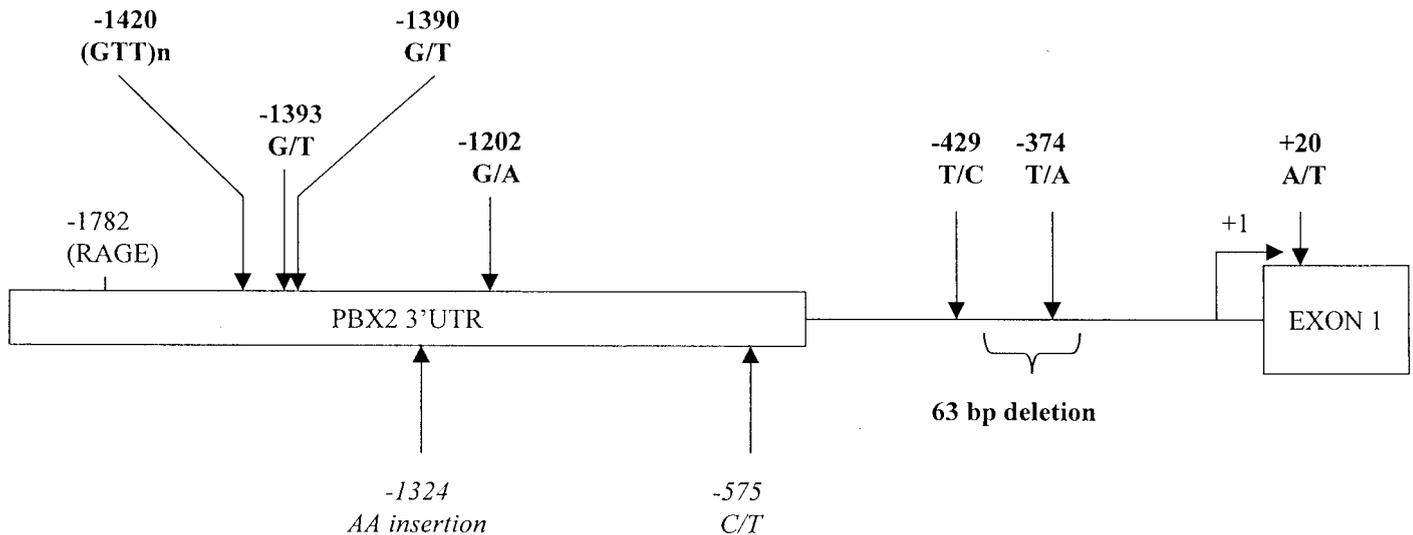
Because of PCR slippage occurring in promoter regions I and J, the RPALL fragment was cloned into a pCR2.1 TOPO vector (Invitrogen), and six clones were picked for each sample and mini-prep purified using Wizard Plus SV Miniprep DNA purification system (Promega). Sequencing reactions were setup using 200 ng of plasmid template with dRhodamine Ready Reaction mix (Applied Biosystems). A wild type RAGE 5′ flanking sequence was then generated from all sequencing results and deposited with Genbank under Accession No. AF208289.

Reporter gene constructs. PCR primers to amplify from −738 to +49 relative to the transcription start site (RAGECATF 5′ CAGCCCTGAACTAGC-TACCAT 3′ RAGECATR 5′ AGCACCCAGGCTCCAACT 3′) were designed because this construct gave the highest basal expression (16). PCR fragments (RAGECAT) were amplified using Expand High Fidelity PCR system as before with a extension of 10 min to A-tail the PCR product to enable cloning into the pCR2.1 TOPO vector (Invitrogen). Five RAGECAT constructs were generated: a wild type for all polymorphisms, a C at −429, an A at −374, a 63-bp deletion from −407 to −345, and a T at +20, as described by Hudson et al. (17). Five clones for each genotype were mini-prep purified as before and sequenced using M13 primers (M13F 5′ GTAAAACGACGGCCAG 3′ M13R 5′ CAGGAAA-CAGCTATGAC 3′) by an automated method, as previously described. Constructs from each genotype were then digested with SacI and XbaI (New England Biolabs) and ligated into a pCAT3-Enhancer vector (Promega) that had been linearized by digestion with SacI and NheI. A total of 10 ng of ligation mix was used to transform DH5α-competent $Escherichia\ coli$ (Life Technologies) that were mini-prep purified as before and plasmid DNA–quantified for transfection.

Transient transfections. A total of 1×10^5 HepG2 cells (ECCAC) were seeded into each well of a six-well plate and grown for 24 h in Minimum Essential Eagle's Medium, supplemented with 10% heat-inactivated fetal calf serum, 2 mmol/l glutamine, and 1% antibiotic/antimycotic solution (Sigma), and incubated at 37°C at 5% CO$_2$. HepG2 cells were transfected with 0.8 µg of each reporter plasmid and 0.2 µg of reporter vector containing the β-galactosidase gene (Promega) using Fugene (Roche) with a 3:1 ratio of liposome reagent–to–plasmid DNA. The cells were incubated for 24 h at 37°C, 5% CO$_2$, to allow expression of reporter genes. Each transfection was performed in duplicate and the experiment was repeated three times.

Quantification of CAT levels. Measurement of CAT and β-galactosidase levels in HepG2 cells was carried out using enzyme-linked immunosorbent assays (Roche). A total of 1 ml of lysis buffer was added to each well of HepG2 cells and incubated for 30 min. Cellular extracts were centrifuged for 15 min at 14,000g at 4°C. Supernatant was removed, and protein concentrations were quantified using the BCA microassay (Pierce). To determine transfection efficiencies, β-galactosidase levels were measured by enzyme-linked immunosorbent assay (Roche) and normalized against measured CAT expression.

EMSA. Sense and antisense oligonucleotides for the −429 T/C (5′-TTTCTT-TCACGAAG[**T/C**]TCCAAACAGGTTTC-3′) and −374 T/A (5′-ATGCAGGC-CCAA[**T/A**]TGCACCCTTGCAGA-3′) polymorphisms were synthesized (Life Technologies). Nuclear protein extracts were prepared from 5×10^6 HepG2 and U937 cells, as previously described (18), and protein yield was quantified by the BCA protein assay (Pierce). EMSA reactions were set up using the Gel Shift assay system (Promega). A total of 100 ng of each sense oligo was labeled with 10 µCi of γ-^{32}P ATP using T4 polynucleotide kinase (Promega) and subsequently double-stranded with 400 ng of respective antisense oligo. End-labeled double-stranded oligos were gel purified from free ATP and single-strand oligo on a 15% acrylamide gel, excised, and eluted in a buffer (500 mmol/l ammonium acetate, 10 mmol/l EDTA). EMSA reactions were set up with 5–10 µg of nuclear protein extract with Gel Shift binding buffer (Promega) and incubated at room temperature for 10 min. For competition assays 1-, 10-, and 100-fold molar excess of specific competitor oligo or 100-fold molar excess of SP1 (Promega) nonspecific competitor oligo was added to the reaction. Then 1 µl of labeled oligonucleotide was added, incubated for 20 min, and electrophoresed on a 4% polyacrylamide gel containing 2.5% glycerol and 0.5 × Tris-Borate-EDTA at 100V for 4 h. The gel was dried and exposed to X-ray film overnight at −70°C.

-1782 (RAGE) **-1420 (GTT)n** **-1393 G/T** **-1390 G/T** **-1202 G/A** **-429 T/C** **-374 T/A** **+20 A/T** **+1** PBX2 3'UTR EXON 1 **63 bp deletion** *-1324 AA insertion* *-575 C/T*

FIG. 1. Map of the RAGE 5′ flanking region with the novel polymorphisms identified. Polymorphisms located on the RAGE gene on chromosome 6 are shown in bold, whereas identified polymorphisms present on the pseudogene of PBX2 are shown in italics.

Restriction fragment–length polymorphism. A restriction fragment–length polymorphism (RFLP) assay was developed to simultaneously screen for the -429 T/C, -374 T/A, and 63-bp deletion. Primers previously used for DHPLC screening to amplify from -590 to -246 (F 5′-GGGGGCAGTTCTCTCCTC-3′ R 5′-TCAGAGCCCCGATCCTATTT-3′) were used for PCR-RFLP. A total of 5 µl of PCR product was electrophoresed on a 1% agarose gel to detect the 63-bp deletion. The remaining PCR product was digested with *Alu* I (New England Biolabs) for 6 h at 37°C followed by overnight digestion with *Tsp*509 I (New England Biolabs) at 65°C. Products were resolved on a 3% agarose gel electrophoresed at 100V for 2 h.

Statistics. Student's *t* test was used to compare levels of CAT activity between constructs, and χ^2 tests were used to determine genotype distribution. All statistical analysis was performed using SPSS version 6.1.

RESULTS

Polymorphisms identified. We examined the occurrence of polymorphisms in the RAGE 5′ flanking region using overlapping PCR regions with SSCP and DHPLC. We identified eight polymorphisms in total (Fig. 1) consisting of the -1420 (GGT)n, -1393 G/T, -1390 G/T, and -1202 G/A in the region overlapping with the PBX2 pseudogene and the -429 T/C, -407 to -345 deletion, -374 T/A, and $+20$ T/A in the single copy region of RAGE. Because of coamplification from both the PBX2 pseudogene (chromosome 3) and PBX2/RAGE (chromosome 6) initially obtained by normal PCR methods and detected by SSCP/DHPLC, two common polymorphisms were identified in regions -1350 to -1156 and -718 to -546 and were later confirmed to be on the PBX2 pseudogene and not on RAGE (Fig. 1).

In addition, in regions -1498 to -1334 and -1350 to -1156, a series of T(n) repeat motifs occurred at positions -1302, -1335, -1426, and -1470. However, by cloning to confirm other polymorphisms within these regions, sequencing confirmed these as PCR artifacts resulting from slippage of *Taq* DNA polymerase (19,20). Because of many discrepancies in Genbank published sequences for RAGE, the nested PCR approach described in RESEARCH DESIGN AND METHODS was used to generate a wild type sequence of RAGE, and the results were deposited in Genbank.

Finally, by using SSCP and DHPLC to analyze the RAGE 5′ flanking region, we were able to compare the two techniques for their relative detection efficiency. All polymorphisms were detected by both methods except for the

common -374 T/A polymorphism, which was detected only by DHPLC and was not detectable under any condition by SSCP. Additionally, the rare 63-bp deletion (which was initially detected by agarose gel electrophoresis when optimizing primers for DHPLC) was not detected by SSCP because this polymorphism overlapped one of the primers used for amplification.

CAT reporter assays. To assess the transcriptional effects of the identified polymorphisms, we constructed an array of CAT reporter gene constructs containing one of the following: wild type, -429 C, -374 A, -407 to -345 deletion, and the $+20$ T nucleotide substitution. The results of these experiments are displayed in Fig. 2 and are the mean of three separate experiments, each performed in duplicate. The relative CAT activity of the constructs containing the -429 C, -374 A, and -407 to -345 deletion were significantly increased compared with that of the wild type CAT activity ($P = < 0.0001$, $P = < 0.0001$, and $P = 0.029$), respectively. CAT activity of the $+20$ T allele was not significantly different from that of the wild type ($P > 0.05$).

EMSA. To further characterize the wild type and mutant forms of the common -374 T/A and -429 T/C polymorphisms, EMSAs were used to detect differences in DNA-nuclear protein interactions in cellular extracts from U937 and HepG2 cells using 29mer double-stranded oligos for each polymorphism. Binding of nuclear protein to the -429 T or C alleles was demonstrated for all cellular extracts (data not shown). Two bands were obtained from both U937 and HepG2 extracts; however, no clear differences were observed between the alleles in terms of nuclear protein binding, with or without competition.

For the -374 T/A polymorphism, a number of specific and nonspecific interactions were demonstrated for both HepG2 and U937 extracts (shown in Fig. 3). With the -374 T probe, a major protein-DNA band was observed (band A in Fig. 3) that was absent with the -374 A probe. In addition, this binding effect was more pronounced in nuclear protein extract from U937s (Fig. 3A) as opposed to HepG2s (Fig. 3B). By performing assays with cold com-
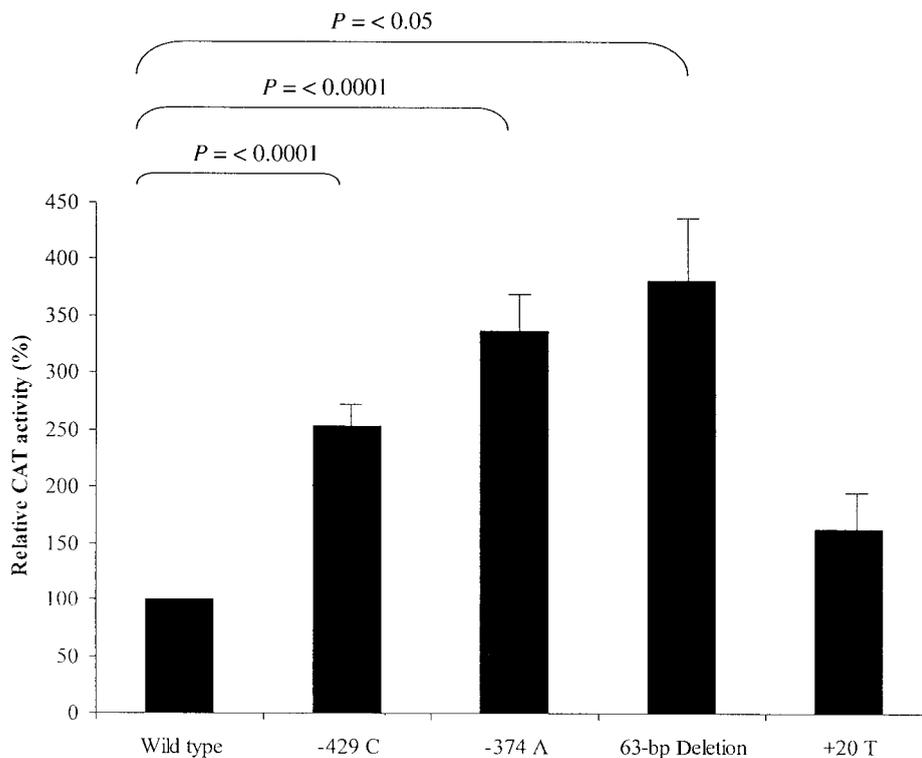
FIG. 2. CAT activity corrected for transfection efficiency and protein yield from transiently transfected HepG2 cells with pCAT inserts, with combinations of polymorphisms identified. The results are expressed as the percentage of the wild type value and are the mean of six experiments.

petitor, this was determined to be a specific interaction because the unlabelled SP1 probe was unable to disrupt this protein-DNA interaction. Further reinforcing that this was an allele-specific binding effect, we found that unlabeled –374 T competitor removed binding to the –374 T probe, whereas the –374 A competitor had no effect on band A (Fig. 3).

RFLP. Using PCR-RFLP, we conducted a preliminary study of the prevalence of the –429 T/C, –374 T/A, and –407 to –345 bp deletion polymorphisms in control and patient groups, with the results presented in Table 1. Because of low numbers of homozygotes for the –429 polymorphism, homozygotes and heterozygotes were combined for analysis for both polymorphisms. We investigated the genotype frequency in type 2 diabetic patients with ($n = 106$) or without ($n = 109$) retinopathy and in nondiabetic control subjects ($n = 113$) (Table 1). There was a significant association between the –429 T/C polymorphism and retinopathy, with those subjects with retinopathy having a higher prevalence of the C allele ($P = 0.012$) (–429 C allele frequency 23.6 vs. 14.9% for those with retinopathy versus those without retinopathy, respectively). There were no significant differences between the –374 T/A polymorphism and retinopathy ($P > 0.05$) or between the control and diabetes groups ($P > 0.05$). The –407 to –345 deletion polymorphism occurred with a genotype frequency of 99% II, 1% ID, and 0% DD in all groups.

Figure 4 shows the RFLP pattern observed when screening for both polymorphisms. This methodology allowed us to obtain complete haplotype data for both polymorphisms. From this data, it can be demonstrated that the –374 A and –429 C alleles do not occur together on the

same DNA strand because a 183-bp band would be obtained by RFLP (Fig. 4A). Further evidence to support this is provided in Table 2, which demonstrates the linkage disequilibrium between these polymorphisms.

DISCUSSION

The identification of increased RAGE expression at sites involved in diabetic vascular complications, in conjunction with accumulated AGE, has implicated RAGE as a candidate gene for vascular disease. The sustained interaction of AGE with RAGE, as seen in diabetes, leads to a prothrombotic and proadhesive state in the endothelium, indicating that RAGE mediates the cellular effects of these toxic moieties. Other studies in transgenic mice have demonstrated the involvement of RAGE in vascular disease by selectively blocking RAGE-binding, leading to a reversal of accelerated atherosclerosis (21).

In this study we investigated the occurrence of polymorphisms in the 5′ regulatory region of RAGE and identified a number of key polymorphisms. We identified eight polymorphisms in total; six single nucleotide polymorphisms (–1393 G/T, –1390 G/T, –1202 G/A, –429 T/C, –374 T/A, +20 T/A), a trinucleotide repeat (–1420 [GGT]n), and a deletion (–407 to –345). The localization of these polymorphisms to the correct loci was complicated by our finding that part of the RAGE 5′ flanking region was duplicated on another chromosome. PBX2, the gene 5′ to RAGE, has its 3′UTR overlapping with part of the RAGE 5′ regulatory region (6). The PBX2 gene has a pseudo-copy on chromosome 3 (22); however, two independent studies using fluorescent in-situ hybridization have shown RAGE to be solely located on chromosome 6 (6,23). To circum-

A

B
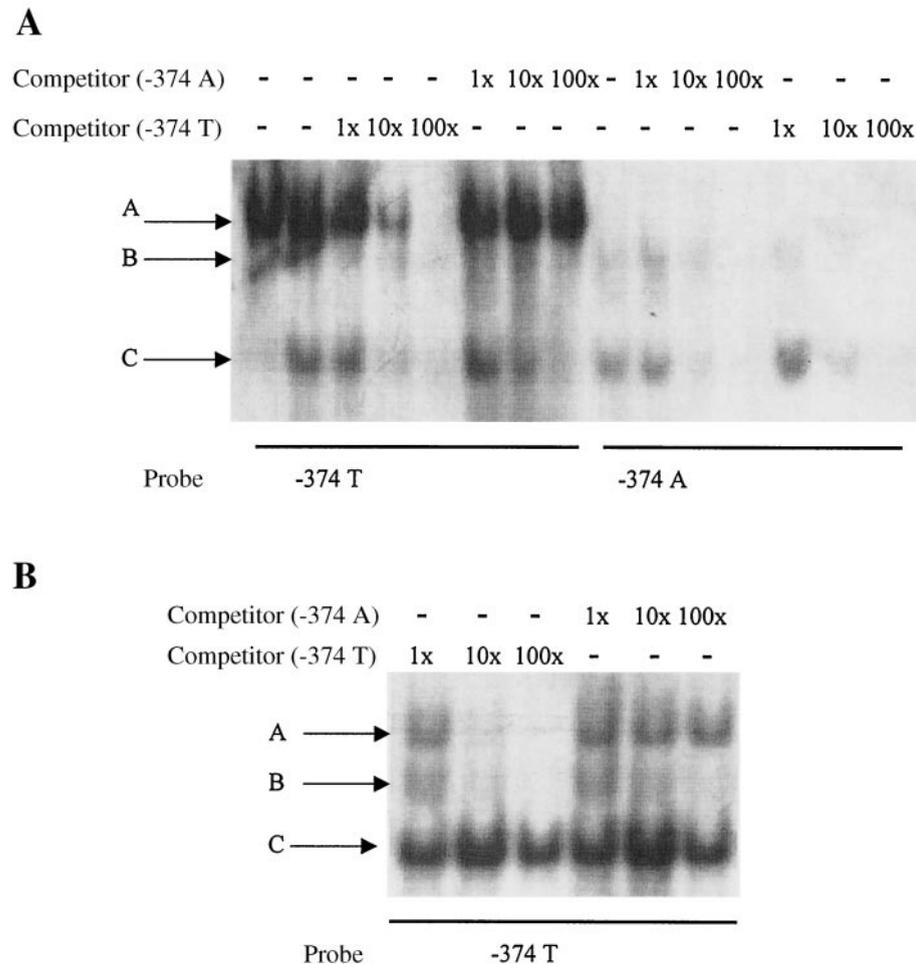
FIG. 3. Electrophoretic mobility shift assays showing binding of nuclear proteins to the –374 T/A polymorphism. Competition is demonstrated using cold self-competitor and SP1 consensus oligonucleotide in excess molar concentrations. Protein-DNA complexes are indicated by arrows. *A*: Protein-DNA complexes formed using U937 nuclear extract. *B*: Protein-DNA complexes formed using HepG2 nuclear extract for the –374T probe to illustrate the allele-specific band A found with U937s.

vent this problem, identified polymorphisms were sequenced using a chromosome 6–specific PCR to confirm their existence at this locus and thus demonstrate a PCR-based methodology that prevents coamplification of duplicated genes.

Once the polymorphisms were characterized, we studied the transcriptional effects of the –429 T/C, –374 T/A, and –407 to –345 deletions and +20 T/A. All of these polymorphisms are in close proximity to the transcrip-

TABLE 1
Genotype frequencies of the −374 and −429 polymorphisms in subjects with type 2 diabetes and in control subjects.

Genotype	Type 2 diabetic subjects with retinopathy	Type 2 diabetic subjects without retinopathy	Control subjects
−374	106	109	113
TT	58.5	60.6	66.5
TA/AA	41.5	39.4	33.5
−429			
TT	56.6	73.3	66.4
TC/CC	43.4	24.7	33.6

Data are %. χ^2 used to determine genotype distribution was P values: –374 retinopathy vs. nonretinopathy, $P > 0.05$; –429 retinopathy vs. nonretinopathy, $P = 0.012$.

tional start site, with both alleles of the −429 T/C and −374 T/A polymorphisms being common. In previous studies on the RAGE 5′ regulatory region, it was found that the −738 to +49 fragment was sufficient and necessary for maximal RAGE expression (16), and hence we used this fragment for our CAT reporter gene studies. The CAT assays revealed that the −429 C and −374 A alleles had a marked effect on transcriptional activity. The effect of these polymorphisms on actual protein-DNA interaction(s) was revealed by subsequent EMSA studies. Although no clear differences were observed for the −429 T/C polymorphism, a very distinct difference in transcription factor binding was observed between the −374 T and A alleles.
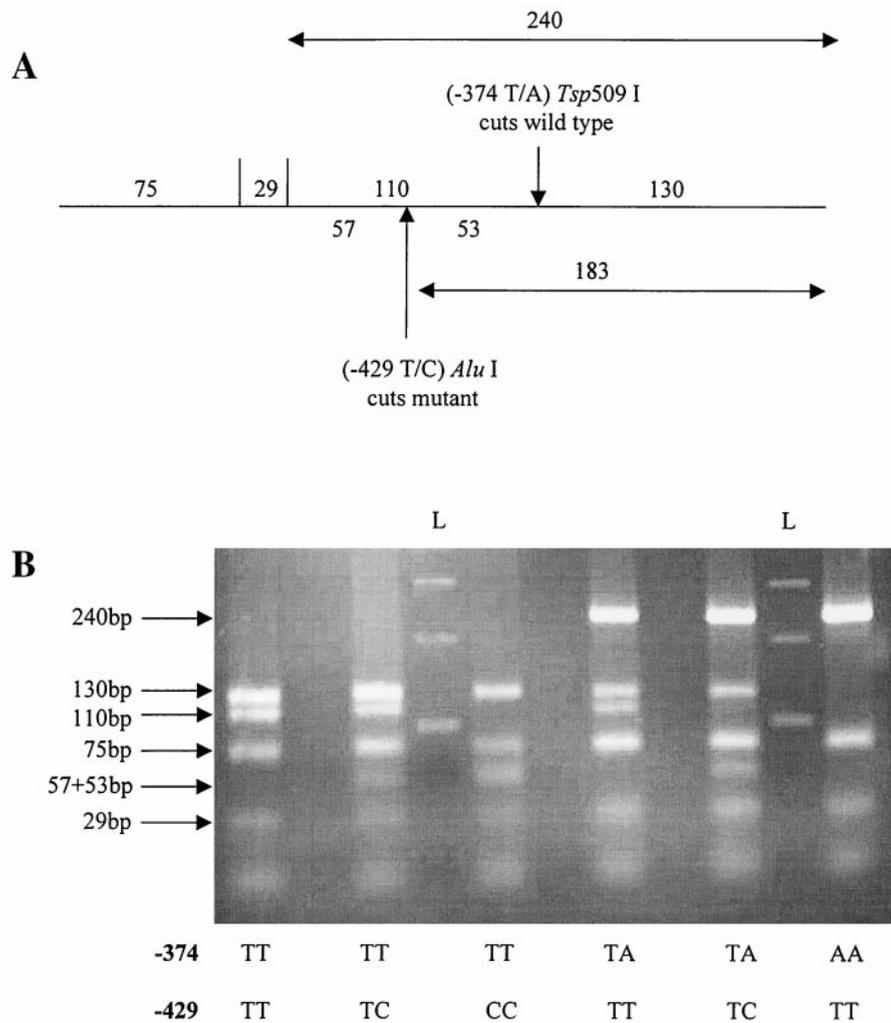
The introduction of the T-to-A nucleotide substitution appeared to prevent the binding of a nuclear binding factor found to form a complex with the –374T probe. This finding, combined with the results for this polymorphism in the reporter gene assays, would suggest that a disruption of a nuclear protein is involved in repression of RAGE transcription. This is further supported by deletion analysis of the RAGE promoter by Li et al. (16), which suggested that a repressor-like domain exists within the –587 to –202 promoter region. If these polymorphisms interfere with such a mechanism, leading to an increase in expression similar to that seen in this study, it is possible that a

FIG. 4. RFLP genotyping of the −374 T/A and −429 T/C polymorphisms. *A*: Restriction endonuclease map of the PCR fragment, with polymorphic sites indicated by arrows. *B*: Result of the gel electrophoresis of digested PCR products on a 3% agarose gel, with each genotype represented.

number of proteins are involved due to the effects of the −429 T/C and 63-bp deletion on reporter gene expression. However, understanding the mechanism(s) responsible for these effects will require the identification of the protein(s) binding within this domain. The nucleotide change at −374 resulting from a T-to-A substitution disrupts the binding of a variety of CTF/NF1 transcription factors established from the TRANSFAC database (24). A number of these proteins have been demonstrated to be involved in negative and positive gene regulation (25). Further studies are thus required to investigate whether these polymorphisms influence increased RAGE expres-

sion and whether this relates to the development of vascular disease in diabetes. To confirm our findings, we intend to identify the factor(s) responsible and their effects. We are currently performing DNaseI footprinting studies to identify the actual binding motif involved, before isolating the protein(s) involved.

We conducted a preliminary study of the prevalence of the −429 T/C and −374 T/A polymorphisms in type 2 diabetic subjects with and without retinopathy and in a nondiabetic control population. The results demonstrated a significant increase of the C allele in subjects with retinopathy compared with those without retinopathy. The −374 T/A polymorphisms were not significantly different between the groups, but they appeared to have a trend toward an increase of the A allele in the retinopathy group. To clarify this relationship, further studies would need to be carried out in larger patient populations.

In summary, we have identified a number of novel polymorphisms within the 5′ regulatory region of the RAGE gene. We investigated effects on transcriptional activity and found an increase in reporter gene expression with the −429 T-to-C, −374 T-to-A, and −407 to −345 deletion polymorphisms. Transcription factor binding assays revealed the abolition of a nuclear protein binding

TABLE 2
Linkage disequilibrium table of the −429 T/C and −374 T/A polymorphisms.

	−429 TT	−429 TC	−429 CC
−374 TT	108	71	11
−374 TA	73	23	0
−374 AA	17	0	0

Data are *n*. D' = 100%, $P < 0.0001$.

site with the introduction of the –374 A allele, supporting the role of these polymorphisms in affecting RAGE transcriptional repression. Furthermore, the C allele of the –429 polymorphism was found to be related to retinopathy in subjects with type 2 diabetes. Further studies are required to evaluate the pathophysiological consequences of the RAGE promoter polymorphisms, specifically as to whether they influence RAGE expression in vivo and whether they have a role in vascular disorders.

ACKNOWLEDGMENTS

REFERENCES

1. Brownlee M: Advanced protein glycosylation in diabetes and aging. *Annu Rev Med* 46:223–234, 1995
2. Brownlee M: Lilly Lecture 1993: Glycation and diabetic complications. *Diabetes* 43: 836–841, 1994
3. Stitt AW, He C, Vlassara H: Characterisation of the advanced glycation end-product receptor complex in human vascular endothelial cells. *Biochem Biophys Res Commun* 256:549–556, 1999
4. Horiuchi S, Higashi T, Ikeda K, Saishoji T, Jinnouchi Y, Sano H, Shibayama R, Sakamoto T, Araki N: Advanced glycation end products and their recognition by macrophage and macrophage-derived cells. *Diabetes* 45 (Suppl. 3):S73–S76, 1996
5. Schmidt AM, Hori O, Brett J, Yan SD, Wautier JL, Stern D: Cellular receptors for advanced glycation end products: implications for induction of oxidant stress and cellular dysfunction in the pathogenesis of vascular lesions. *Arterioscler Thromb* 14:1521–1528, 1994
6. Sugaya K, Fukagawa T, Matsumoto KI, Mita K, Takahashi EI, Ando A, Inoko H, Ikemura T: Three genes in the human MHC class II region near the junction with the class II: gene for receptor of advanced glycosylation end products, PBX2 homeobox gene and a notch homolog, human counterpart of mouse mammary tumor gene int-3. *Genomics* 23:408–419, 1994
7. Brett J, Schmidt AM, Yan SD, Zou YS, Weidman E, Pinsky D, Nowygrod R, Neeper M, Przysiecki C, Shaw A, Migheli A, Stern D: Survey of the distribution of a newly characterized receptor for advanced glycation end products in tissues. *Am J Pathol* 143:1699–1712, 1993
8. Soulis T, Thallas V, Youssef S, Gilbert RE, McWilliam BG, Murray-McIntosh RP, Cooper ME: Advanced glycation end products and their receptors co-localise in rat organs susceptible to diabetic microvascular injury. *Diabetologia* 40:619–628, 1997
9. Ritthaler U, Deng Y, Zhang Y, Greten J, Abel M, Sido B, Allenberg J, Otto G, Roth H, Bierhaus A, Ziegler R, Schmidt AM, Waldherr R, Wahl P, Stern DM, Nawroth PP: Expression of receptors for advanced glycation end products in peripheral occlusive vascular disease. *Am J Pathol* 146:688–694, 1995
10. Schmidt AM, Yan SD, Wautier JL, Stern D: Activation of receptor for advanced glycation end products: a mechanism for chronic vascular dysfunction in diabetic vasculopathy and atherosclerosis. *Circ Res* 84:489–497, 1999
11. Bierhaus A, Illmer T, Kasper M, Luther T, Quehenberger P, Tritschler H, Wahl P, Ziegler R, Muller M, Nawroth PP: Advanced glycation end product (AGE)-mediated induction of tissue factor in cultured endothelial cells is dependent on RAGE. *Circulation* 96:2262–2271, 1997
12. Yamagishi S, Fujimori H, Yonekura H, Yamamoto Y, Yamamoto H: Advanced glycation endproducts inhibit prostacyclin production and induce plasminogen activator inhibitor-1 in human microvascular endothelial cells. *Diabetologia* 41:1453–1441, 1998
13. Schmidt AM, Yan SD, Brett J, Mora R, Nowygrod R, Stern D: Regulation of human mononuclear phagocyte migration by cell surface-binding proteins for advanced glycation end products. *J Clin Invest* 91:2155–2168, 1993
14. Nagi DK, Mansfield MW, Stickland MH, Grant PJ: Angiotensin converting enzyme (ACE) insertion/deletion (I/D) polymorphism and diabetic retinopathy in subjects with IDDM and NIDDM. *Diabet Med* 12:997–1001, 1995
15. Sanguinetti CJ, Neto ED, Simpson AJG: Rapid silver staining and recovery of PCR products separated on polyacrylamide gels. *Biotechniques* 17:915–919, 1994
16. Schmidt AM, Li J: Characterisation and functional analysis of the promoter of RAGE, the receptor for advanced glycation end products. *J Biol Chem* 272:16498–16506, 1997
17. Hudson BI, Stickland MH, Grant PJ: Identification of polymorphisms in the receptor for advanced glycation end-products (RAGE) gene: prevalence in type 2 diabetes mellitus and ethnic groups. *Diabetes* 47:1155–1157, 1998
18. Andrews NC, Faller DV: A rapid micropreparation technique for extraction of DNA-binding proteins from limiting numbers of mammalian cells. *Nucleic Acids Res* 19:2499, 1991
19. Meldgaard M, Morling N: Detection and quantitative characterization of artificial extra peaks following polymerase chain reaction amplification of 14 short tandem repeat systems used in forensic investigations. *Electrophoresis* 18:1928–1935, 1997
20. Ji JP, Clegg NJ, Peterson KR, Jackson AL, Laird CD, Loeb LA: In vitro expansion of GGC:GCC repeats: identification of the preferred strand of expansion. *Nucleic Acids Res* 24:2835–2840, 1996
21. Park L, Raman KG, Lee KJ, Lu Y, Ferran LJ, Chow WS, Stern D, Schmidt AM: Suppression of accelerated diabetic atherosclerosis by the soluble receptor for advanced glycation endproducts. *Nat Med* 4:1025–1031, 1998
22. Aguado B, Campbell RD: The novel gene G17, located in the human major histocompatibility complex, encodes PBX2, a homeodomain-containing protein. *Genomics* 25:650–659, 1995
23. Vissing H, Aagaard L, Tommerup N, Boel E: Localization of the human gene for advanced glycosylation end product-specific receptor (AGER) to chromosome 6p21.3. *Genomics* 24:606–608, 1994
24. Knuppel R, Dietze P, Lehnberg W, Frech K, Wingender E: TRANSFAC retrieval program: a network model database of eukaryotic transcription regulating sequences and proteins. *J Comput Biol* 3:191–198, 1994
25. Roulet E, Bucher P, Schneider R, Wingender E, Dusserre Y, Werner T, Mermod N: Experimental analysis and computer prediction of CTF/NF1 transcription factor DNA binding sites. *J Mol Biol* 297:833–848, 2000